Diel light cycles affect phytoplankton competition in the global ocean

Citation: Tsakalakis, Ioannis, Follows, Michael J, Dutkiewicz, Stephanie, Follett, Christopher L and Vallino, Joseph J. 2022. "Diel light cycles affect phytoplankton competition in the global ocean." Global Ecology and Biogeography, 31 (9).

As Published: 10.1111/geb.13562

Publisher: Wiley

Persistent URL: https://hdl.handle.net/1721.1/145706

Version: Final published version: final published article, as it appeared in a journal, conference proceedings, or other formally published context

Received: 19 May 2021 | Revised: 11 April 2022 | Accepted: 10 June 2022

DOI: 10.1111/geb.13562

Global Ecology and Biogeography A Journal of Macroecology WILEY

RESEARCH ARTICLE

Diel light cycles affect phytoplankton competition in the global ocean

Ioannis Tsakalakis[1,2] | Michael J. Follows[2] | Stephanie Dutkiewicz[2] | Christopher L. Follett[2] | Joseph J. Vallino[1]

[1]Ecosystems Center, Marine Biological Laboratory, Woods Hole, Massachusetts, USA

[2]Department of Earth, Atmospheric and Planetary Sciences, Massachusetts Institute of Technology, Cambridge, Massachusetts, USA

Correspondence
Ioannis Tsakalakis, Marine Biological Laboratory, Woods Hole, MA 02543, USA.
Email: itsakalakis@mbl.edu

Funding information
National Science Foundation, Grant/Award Number: 1841599, DEB-1655552, OCE-1558710 and OCE-1637630; Simons Foundation, Grant/Award Number: CBIOMES #549931, CBIOMES #549941, CBIOMES #553242 and CBIOMES #827829

Handling Editor: Aaron MacNeil

Abstract

Aim: Light, essential for photosynthesis, is present in two periodic cycles in nature: seasonal and diel. Although seasonality of light is typically resolved in ocean biogeochemical–ecosystem models because of its significance for seasonal succession and biogeography of phytoplankton, the diel light cycle is generally not resolved. The goal of this study is to demonstrate the impact of diel light cycles on phytoplankton competition and biogeography in the global ocean.

Location: Global ocean.

Major taxa studied: Phytoplankton.

Methods: We use a three-dimensional global ocean model and compare simulations of high temporal resolution with and without diel light cycles. The model simulates 15 phytoplankton types with different cell sizes, encompassing two broad ecological strategies: small cells with high nutrient affinity (gleaners) and larger cells with high maximal growth rate (opportunists). Both are grazed by zooplankton and limited by nitrogen, phosphorus and iron.

Results: Simulations show that diel cycles of light induce diel cycles in limiting nutrients in the global ocean. Diel nutrient cycles are associated with higher concentrations of limiting nutrients, by 100% at low latitudes (−40° to 40°), a process that increases the relative abundance of opportunists over gleaners. Size classes with the highest maximal growth rates from both gleaner and opportunist groups are favoured by diel light cycles. This mechanism weakens as latitude increases, because the effects of the seasonal cycle dominate over those of the diel cycle.

Main conclusions: Understanding the mechanisms that govern phytoplankton biogeography is crucial for predicting ocean ecosystem functioning and biogeochemical cycles. We show that the diel light cycle has a significant impact on phytoplankton competition and biogeography, indicating the need for understanding the role of diel processes in shaping macroecological patterns in the global ocean.

KEYWORDS
biogeography, diel light cycle, global ocean, modelling, nutrient cycles, phytoplankton, resource competition

1 | INTRODUCTION

Marine phytoplankton drive photosynthesis and biogeochemical cycles in the ocean, affecting ocean productivity and the climate of the Earth. They constitute a polyphyletic group characterized by a tremendous number of species differing in forms and functions (Litchman & Klausmeier, 2008) and spanning more than seven orders of magnitude in cell volume (Finkel et al., 2010). Although the geographical distribution, or biogeography, of phytoplankton species is still relatively sparsely mapped in the global ocean, major phytoplankton functional groups (e.g., cyanobacteria, diatoms and dinoflagellates) and size classes appear to have distinct differences in biogeography (Barton et al., 2013). An understanding of the environmental and ecological factors controlling phytoplankton biogeography is an important element linking community structure with ocean productivity, stability and resilience to environmental stressors (Ptacnik et al., 2008; Winder & Sommer, 2012). Predicting the biogeography of phytoplankton size classes is particularly important for climate change predictions, given that large phytoplankton (such as diatoms) have higher sinking rates compared with their smaller counterparts (such as small cyanobacteria), enhancing carbon sequestration from the surface to the deep ocean (Tréguer et al., 2018).

To help understand the role of diverse phytoplankton and their biogeography, ocean ecologists have experimentally derived and constrained parameters that govern the traits and trade-offs of phytoplankton (Finkel et al., 2010; Litchman & Klausmeier, 2008), and these parameters are the foundations for marine ecosystem models (Follows & Dutkiewicz, 2011). Such models have been incorporated into global ocean circulation models to describe general patterns of phytoplankton functional biogeography, including the preponderance of gleaners and opportunists (Aumont et al., 2003; Chai et al., 2007; Dutkiewicz et al., 2009), and the realized niche of nitrogen fixers (Dutkiewicz et al., 2014; Follett, Dutkiewicz, et al., 2018; Landolfi et al., 2015) or mixotrophic plankton (Ward & Follows, 2016). Such models have also been used to derive mechanistic explanations for the structure of plankton food webs (Prowe et al., 2012; Ward et al., 2012), biodiversity patterns in the global ocean (Barton et al., 2010; Dutkiewicz et al., 2020; Vallina et al., 2014) and the impact of climate change in marine ecosystems (Dutkiewicz et al., 2015, 2019).

An important environmental factor considered by the majority of ocean models is the seasonal light cycle (Sommer et al., 2012), because it controls the dynamics of competition between phytoplankton gleaners and opportunists. Gleaners are the pico-phytoplankton (e.g., small cyanobacteria) that exhibit a high affinity for nutrient uptake, whereas opportunists are fast-growing nano-phytoplankton (e.g., diatoms) that have high maximal growth rates (μ_{max}). During spring at temperate latitudes, availability of both light and nutrients leads to the typical spring bloom period when phytoplankton biomass increases rapidly until nutrients are depleted and limit phytoplankton growth in summer. Although seasonal dynamics and initiation of the spring bloom can be controlled by several factors (Behrenfeld & Boss, 2014), the above mechanism describes a major part of phytoplankton seasonal succession, whereby opportunistic phytoplankton dominate during the resource-replete spring bloom period and phytoplankton gleaners prevail in the nutrient-depleted conditions in summer. Given that seasonality becomes stronger with latitude, ocean models predict an increase in fitness of opportunistic phytoplankton in temperate and polar regions (Dutkiewicz et al., 2009; Follows et al., 2007; Tsakalakis et al., 2018), in agreement with observed patterns in the abundance of diatoms and picocyanobacteria (Acevedo-Trejos et al., 2013; Bracher et al., 2009; Flombaum et al., 2013; Hirata et al., 2011).

The diel cycle is the other time scale over which light fluctuates periodically; however, research is limited regarding its effects on phytoplankton biogeography. Resource competition theory suggests that gleaner types should always dominate in a system where resource oscillations are absent or weak (Grover, 1990; Tilman, 1982). Their high nutrient affinity allows them to draw down limiting nutrients to levels where other strategies might not be competitive. However, in the presence of an environment-driven resource oscillation, such as the seasonal cycle, opportunistic types have an advantage during phases of high resource availability based on their higher maximal growth rates (Grover, 1990). Theoretical models have also shown that diel cycles of light or nutrients favour opportunistic phytoplankton (Litchman & Klausmeier, 2001), supported by experimental observations (Litchman, 1998, 2003; Litchman et al., 2004). In a previous modelling study, we explored the effects of diel light cycles on nutrient concentrations and phytoplankton competition in a simple chemostat system (Tsakalakis et al., 2018). It was shown that diel light cycles can induce nutrient oscillations that favour opportunistic phytoplankton over gleaners in a similar manner to the impact of seasonality.

Here, we examine the implications of this process in the more complex setting of a global ocean simulation. We ask, to what extent do diel light cycles impact the emergent large-scale biogeography of phytoplankton? We hypothesize that the mechanisms of the idealized study will carry through, but also consider how a more complex physical environment and ecosystem structure affect the outcome. We study the effects of diel light cycles in a three-dimensional global ocean circulation and biogeochemical model (Dutkiewicz et al., 2021). The model simulates dynamics of a diverse phytoplankton community limited by nitrogen, phosphorous and iron and preyed upon by zooplankton. The model results show that diel light cycles induce diel oscillations of limiting nutrients in the global ocean that increase the relative abundance of fast-growing phytoplankton types, in agreement with the conceptual study by Tsakalakis et al. (2018). Our study indicates that diel light cycles do affect nutrient dynamics and gleaner–opportunist competition and suggests that accounting for diel cycles should improve predictions of marine microbial dynamics and biogeography.

2 | METHODS

The physics of the global ocean model is based on the MITgcm model (Marshall et al., 1997), and the biogeochemical–ecosystem model follows Dutkiewicz et al. (2021), with some modifications that are discussed below. Of significance here, light input is configured to resolve diel cycles and compared with a control simulation without diel light variations.

We use a configuration of the MITgcm ocean model that simulates global ocean circulation, constrained to be consistent with altimetric and hydrographic observations (the ECCO-GODAE state estimates; Wunsch & Heimbach, 2007). It has a horizontal resolution of 1°×1° and 23 vertical levels that span from the surface to a maximal depth of 5,700 m, with level thickness ranging from 10 m near the surface to 500 m at depth. The coupled biogeochemical–ecosystem model resolves the cycling of carbon, nitrogen, phosphorus, iron and oxygen through inorganic, living, particulate and dissolved organic constituents. It resolves 15 phytoplankton types differing in size and biogeochemical function and 15 size classes of zooplankton. Phytoplankton types are spaced uniformly in log space from 0.6 to 228 μm equivalent spherical diameter (ESD) and grouped into two functional groups: the four smallest are gleaners (0.6–2.0 μm ESD), whereas the remaining 11 are opportunists (3.0–155 μm ESD). For ease in interpretation, our model community is simplified in comparison to the study by Dutkiewicz et al. (2021); the gleaners are analogues of pico-cyanobacteria and pico-eukaryotes, whereas the opportunists are based on diatom growth parameters, except that they are not limited by silica here.

Phytoplankton parameters such as maximal growth rate, affinity for nutrient uptake, grazing by zooplankton and sinking are parameterized as a power-law function of cell volume informed by compilations of phytoplankton growth parameters (Dutkiewicz et al., 2020; Ward et al., 2012). Phytoplankton maximal specific growth rates have a unimodal relationship with cell size, peaking at intermediate sizes, in agreement with experimental observations (Dutkiewicz et al., 2020; Finkel et al., 2010; Marañón et al., 2013; Raven, 1994; Sommer et al., 2017); phytoplankton <3 μm have an increase in specific growth rate with size, whereas those >3 μm have a decrease in specific growth rate with size. It is also assumed that affinity for nutrient uptake decreases with cell size; the smallest phytoplankton have the highest affinity for nutrient uptake (Edwards et al., 2012) based on their higher surface-area-to-volume ratio (Kiørboe, 1993; Raven, 1994).

The model uses Monod kinetics to describe nutrient-dependent growth of phytoplankton (Monod, 1949), while C, N, P and Fe requirements are constant but different among functional groups. Chlorophyll *a* for each phytoplankton type is variable and dependent on light and nutrient availability, following the study by Geider et al. (1998). Zooplankton grazing is resolved using a Holling type III grazing function (Holling, 1959) for 15 zooplankton size classes (from 6.6 to 1635 μm ESD) that graze on phytoplankton 10 times smaller than themselves. Maximal grazing rate decreases with size following the study by Hansen et al. (1997). In the paper by Dutkiewicz et al. (2021), each zooplankton size class can prey upon several phytoplankton size classes in addition to other zooplankton smaller than themselves. Here, we use a simplified grazing function, whereby a given zooplankton size class grazes upon a single phytoplankton size class that is 10 times smaller than itself. However, two additional grazing configurations were tested to ensure the robustness of the model: (1) whereby zooplankton graze on several phytoplankton; or (2) whereby zooplankton graze on several phytoplankton in addition to zooplankton (i.e., carnivory) that are 5–20 times smaller than the grazer, but preferentially 10 times smaller. The last grazing scenario follows that in the paper by Dutkiewicz et al. (2021).

Two light regimes were considered: a control simulation, with only seasonal light cycles, and a diel simulation, with both seasonal and diel light cycles. In the control simulation, monthly averaged irradiance levels in the surface ocean were provided by the Ocean–Atmosphere Spectral Irradiance Model (OASIM), which includes the impact of clouds, water vapour and aerosols in the atmosphere, as used by Dutkiewicz et al. (2020), but here we sum the different light wavelengths, providing a single dimension of photosynthetically active radiation (PAR). Given that the simulations of the present study have much higher temporal resolution (3-hour time step) than the monthly averaged irradiance input, a linear interpolation is used to provide a smooth transition of PAR. In the diel simulation, Brock's (1981) system of equations was used to produce surface light fields with high temporal resolution. Brock's equations calculate diel cycles of light intensity and changes in day length across the surface of the globe, unperturbed by cloud formation or other processes. The light field with diel cycles was then normalized to match the annual average irradiance of the control simulation. This ensured that the two simulations have the same light energy input on average, allowing for a fair comparison between them. Additionally, we tested simulations with daily averaged irradiance as an intermediate scenario between the control and diel simulations. However, it is not used in the present analysis because it produces almost identical results to the control simulation in terms of plankton biogeography. Model runs of 10 years with a time step of three steps per hour were used, and test runs of 20 years ensured that the 10-year runs were sufficient for reaching a quasi-steady state in terms of plankton biogeography, which was typically achieved between the first 2–5 years of the model. The last simulated year was used to analyse annually averaged patterns and annual and diel dynamics of model variables.

When using the same growth parameter values in both control and diel simulations, the diel case led to substantially lower primary production (PP). The average of a nonlinear function (the diel simulation in this case) is not usually equal to the nonlinear function with averaged input (the control simulation), as described by Jensen's inequality (Denny, 2017; Jensen, 1906). Particular to our model analysis, nighttime increased phytoplankton mortality in the diel simulation, and the higher light intensity during the day (compared with the control simulation) could not compensate for nighttime losses because the growth rate saturated or diminished at high light intensity. To match PP of the diel simulation to the control simulation, we increased maximal specific growth rates of all phytoplankton types by a factor of 1.83 (we investigated several factors and chose the factor that matched the PP of the control simulation; see Supporting Information Figure S1). With this alteration in the diel simulation, other model variables, such as plankton biomass and limiting nutrients, also approached concentrations found in the control simulation (Supporting Information Figure S1). However, owing to Jensen's inequality, the best match of other variables required different μ_{max} factors (e.g., phytoplankton biomass matched the control when using a μ_{max} factor = 1.65). We have provided model results for several μ_{max} factors in the Supporting Information Figure S7, supporting the robustness of the proposed ecological mechanisms.

To illustrate the effect of diel light cycles on limiting nutrient concentrations, we used the following metric:

$$\text{Diel effect percentage (on concentration)} = 100\frac{Diel_N - Control_N}{Control_N}, \quad (1)$$

where $Diel_N$ and $Control_N$ are the concentrations of nutrient N in diel and control simulations, respectively. This metric was used to show the percentage change of nutrient concentrations when diel light cycles were used in the model. We used a different metric to illustrate changes in species composition, which showed the effect of diel cycles on phytoplankton relative abundances:

$$\text{Diel effect percentage (on relative abundance)} = 100\left(\frac{Diel_P}{Diel_{total}} - \frac{Control_P}{Control_{total}}\right), \quad (2)$$

where $Diel_P$ and $Control_P$ are biomass concentrations of phytoplankton type/group P, and $Diel_{total}$ and $Control_{total}$ are the total phytoplankton biomasses in the diel and control simulations, respectively.

3 | RESULTS

The model captures the patterns of high productivity in the equatorial and subpolar regions and the oligotrophic conditions in subtropical gyres (Supporting Information Figure S2; model results can be retrieved online; Tsakalakis et al., 2021), in addition to the typical global surface distribution of limiting nutrients (Figure 1a–c). Dissolved inorganic nitrogen (DIN = $NO_3^- + NO_2^- + NH_4^+$) has low concentrations in the Indian and Atlantic Oceans and in the subtropics of the Pacific Ocean (Figure 1a). Low concentrations of phosphate follow a similar pattern to DIN (Figure 1b), while both DIN and PO_4^{3-} are in excess in the Southern Ocean, which is known to be limited primarily by iron and light (Thomas, 2003). Iron exhibits low concentrations in the Pacific and Southern Oceans, whereas it reaches high concentrations in the Indian and Atlantic Oceans (Figure 1c).

Diel light cycles increase the concentration of the most limiting nutrient at low latitudes. We focus on model results of the surface ocean (0–55 m depth), because the diel cycles are restricted to the surface (Supporting Information Figure S2). Overall, significant increases of nutrient concentrations attributable to diel light cycles are present at low latitudes (−40° to 40°). DIN concentrations increase by ≤100% in regions where DIN has its lowest concentration in the

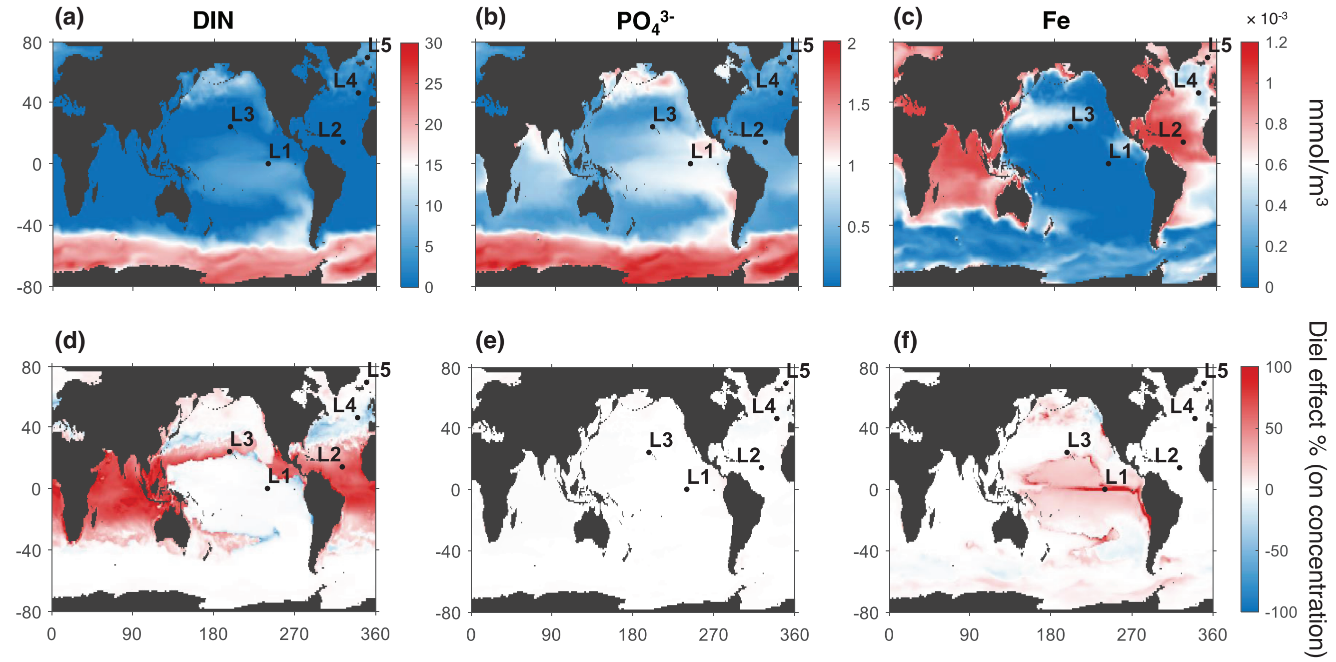

FIGURE 1 Effect of diel light cycles on concentrations of limiting nutrients. The top panels show annually averaged surface (0–55 m depth) nutrient concentrations in the control simulation, and the bottom panels show the effect of diel light cycles compared with the control simulation (Equation 1; difference in concentrations between diel and control, divided by the control, expressed as a percentage). Dissolved inorganic nitrogen (DIN) refers to the sum of NO_3^-, NO_2^- and NH_4^+. Labelled black dots indicate locations (L1–L5) for which annual dynamics are presented in Figure 2.

control simulation (i.e., low latitudes in Indian and Atlantic Oceans and subtropics of the Pacific; Figure 1d). Fe concentrations increase significantly (also by ≤100%) in the Pacific Ocean, especially at low latitudes (Figure 1f). Note that the patterns of increased concentrations of DIN and Fe are complementary (i.e., only a single nutrient increases locally). Calculation of nutrient limitation for gleaner and opportunist types shows that the distribution of DIN and Fe limitation coincides with the increases of those nutrients in the diel simulation (Supporting Information Figure S3), supporting that the diel light cycles increase the local concentration of the most limiting nutrient. In contrast, PO_4^{3-} concentrations are not affected by diel light cycles (Figure 1e), because PO_4^{3-} is not the most limiting nutrient at any low-latitude region in the model (Supporting Information Figure S3). Note that PO_4^{3-} can be a major limiting nutrient at low latitudes too, especially for diazotrophic phytoplankton in the subtropical Atlantic (Monteiro et al., 2010), but we do not consider diazotrophs here.

We present model time series of five ocean locations (Figure 2) ranging from low latitudes (L1–L3; locations are shown in Figure 1) to a temperate (L4) and a polar location (L5). PAR exhibits (according to the experimental design) only seasonal cycles in the control simulation (red lines in Figure 2, row 1) and both seasonal and diel cycles in the diel simulation (grey lines in Figure 2, row 1). Note that what appear to be grey shaded areas in Figure 2 are attributable to diel oscillations. At low-latitude locations, L1–L3, diel cycles in PAR (Figure 2a1–a3) induce pronounced diel oscillations throughout the year in PP (Figure 2b1–b3). Furthermore, there are strong oscillations

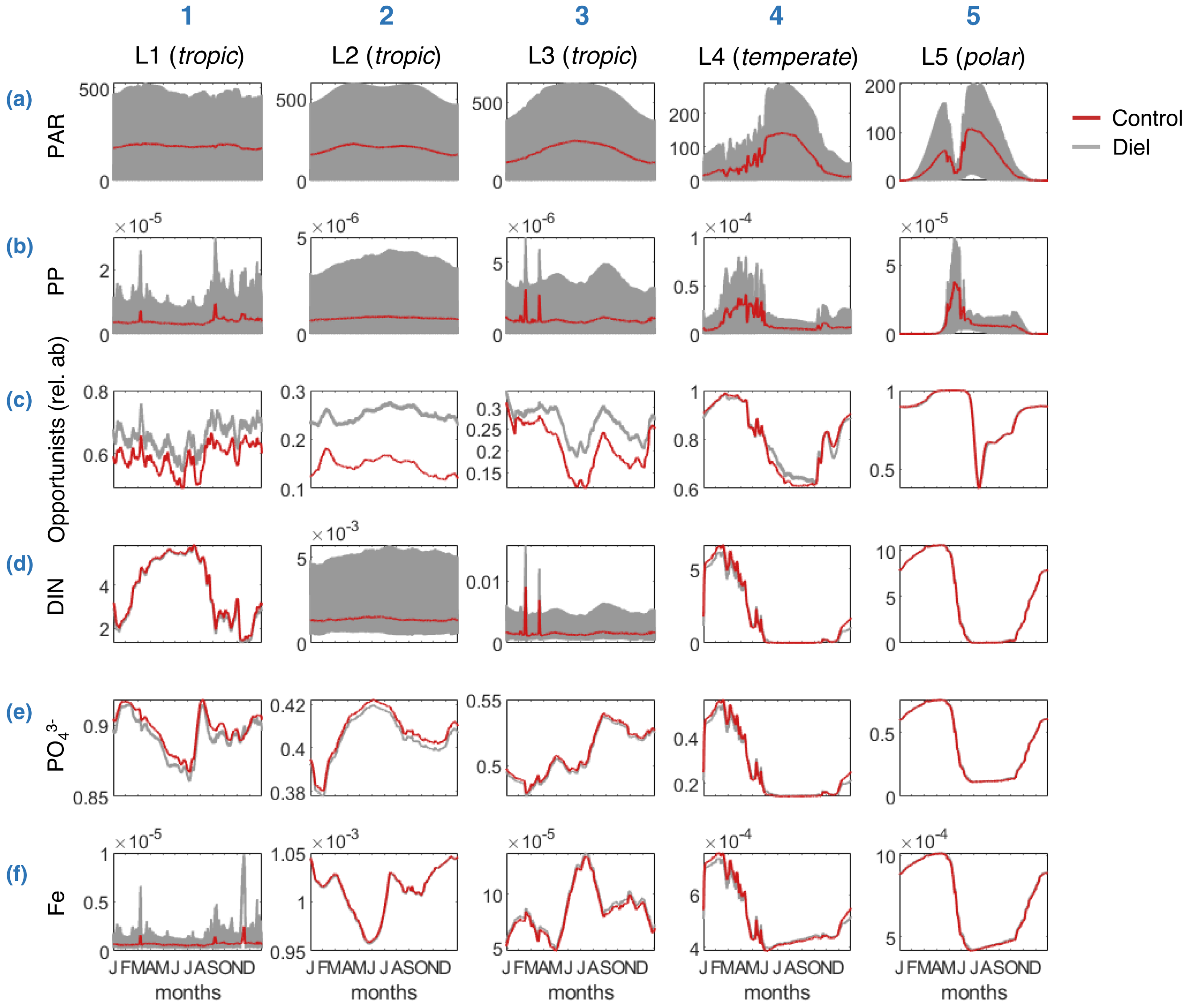

FIGURE 2 Annual dynamics in the control (red) and diel (grey) simulations of: (a) photosynthetically active radiation (PAR; in microensteins per metre squared per second); (b) primary production (PP; in millimoles of carbon per metre cubed per second); (c) relative abundance of opportunists; (d) dissolved inorganic nitrogen (DIN) = $NO_3^- + NO_2^- + NH_4^+$ (in millimoles of nitrogen per metre cubed); (e) PO_4^{3-} (in millimoles of phosphorus per metre cubed); and (f) Fe (in millimoles of iron per metre cubed) at five locations of the surface ocean (averaged from 0 to 55 m depth). Locations (L1–L5) are illustrated in Figure 1. Note that grey shaded areas are attributable to diel oscillations.

and higher averaged concentrations on the most limiting nutrient; strong Fe diel oscillations in location L1 (Figure 2f1), and DIN oscillations in locations L2 and L3 (Figure 2d2 and d3, respectively). Those diel cycles of limiting nutrients in the tropics are associated with an increase in the relative abundance of opportunists (Figure 2c1–c3).

Dynamics at higher latitudes (locations L4 and L5) show that the impact of seasonality dominates over the effects of diel light cycles; nutrient levels are very similar between control and diel simulations (Figure 2, columns 4 and 5), oscillating strongly at a seasonal scale. Although diel nutrient cycles are still present at temperate and polar locations in the diel simulation, they are barely discernable in the figures, because seasonal oscillations are much larger in amplitude. Several locations at temperate latitudes across the global map support the same result (Supporting Information Figures S4 and S5). That is why the relative abundance of opportunists is very similar between control and diel simulations at high latitudes; however, they increase weakly during summer months, indicating the impact of diel light cycles during limiting nutrient conditions, in a similar manner to the mechanism occurring in tropics (Figure 2; Supporting Information Figure S4 and S5).

The diel cycle in limiting nutrients (Figure 3c) is a result of cessation of photosynthesis (and nutrient uptake in our Monod-based model) during the night, but with the continuation of remineralization of detrital matter. During the daytime, phytoplankton nutrient uptake rapidly decreases the concentration of the limiting nutrient, which increases again during the night. This mechanism of nutrient accumulation at night maintains the higher average concentrations of the most limiting nutrient in the diel simulation (Figure 1). PAR and PP also have a strong diel pattern in the diel simulation, as expected (Figure 3a,b). Note that PAR decreases slightly during the day, based on the increasing phytoplankton biomass that absorbs light (grey line in Figure 3a), and PP also declines rapidly during the daytime based on the increased nutrient limitation (grey line in Figure 3b).

The biogeography of gleaners and opportunists in the control simulation follows a similar pattern to that in previous studies, with the biomass of gleaners distributed more uniformly across the global ocean (Figure 4a), while opportunists have low concentrations in the tropics, but substantially increased biomass in temperate and subpolar regions (Figure 4b). Note that the areas with the presence of ice are masked out (white with hatching) because the phytoplankton biomass underneath ice is generally at very low concentrations and sensitive to our diagnostics. Addition of diel light cycles to the model increases the relative abundance of opportunists compared with the control simulation (Figure 4d), a pattern that is restricted to low latitudes, where significant diel cycles in limiting nutrients are present. The increased fitness of opportunists at low latitudes is associated with the decline in relative abundance of gleaners (Figure 4c).

Analysis of changes in relative abundances associated with diel light cycles of the 15 phytoplankton types indicates that fast-growing size classes are favoured at low latitudes (Figure 5a,b). Note that the largest gleaners and the smallest opportunists have the highest maximal growth rates among their groups. In tropical regions of both the Southern and Northern Hemispheres, the relative abundance of small opportunists increases in the diel simulation compared with the control simulation (red circles in Figure 5a,b), a pattern that disappears at temperate latitudes (Figure 5c,d). The relative abundance of gleaners decreases in the tropics across all four gleaner types. However, the largest gleaners, which have the highest maximal specific growth rate among gleaners, are affected less negatively. Overall, Figure 5 illustrates that diel light cycles favour fast-growing types from both gleaner and opportunist groups at low latitudes, where diel cycles in limiting nutrients are present.

Further model analysis was used to test the robustness of the proposed diel mechanism. The increased relative abundance of opportunists over gleaners persists when considering phytoplankton abundances of deeper waters, averaged from 0 to 360 m (Supporting Information Figure S6). The same result holds for different μ_{max} factors tested: from 1.00, where growth parameters in the diel simulation are same as in the control, to 1.65, which matches with the control in phytoplankton biomass, 1.83, which matches with the control in PP, and 2.20, which leads to the best fit on DIN and Fe concentrations between diel and control simulations (Supporting Information Figure S7).

The dominance of opportunists attributable to the introduction of diel cycles is significantly stronger when zooplankton are removed from the model (Supporting Information Figure S8a); opportunists outcompete gleaners in all productive ocean regions where the diel nutrient cycles are the strongest. Also, only the smallest gleaner (best nutrient competitor) and the smallest opportunist (fastest growing type) survive in the absence of zooplankton, where bottom-up effects are the only controls on the outcome of competition. Opportunists are also favoured by diel cycles when using more complex predation functions, such as when zooplankton prey upon several phytoplankton (Supporting Information Figure S8b) or on several phytoplankton and other zooplankton (Supporting Information Figure S8c) smaller than themselves. However, these grazing configurations lead to stronger top-down control and weaker diel effects, although the latter are still present.

4 | DISCUSSION

Global ocean models aim to capture large-scale patterns of community structure and ocean biogeochemistry. To achieve that, the essential environmental factors should be considered. The goal of the present study was to demonstrate the role of the diel light cycle on nutrient dynamics and phytoplankton competition in the global ocean. Although experimental studies have shown that diel light cycles select for opportunistic phytoplankton (Litchman, 1998, 2003; Litchman et al., 2004), experimental evidence of diel nutrient cycles is lacking. Our previous work showed that the diel light cycle induces significant cycles in limiting nutrients in a chemostat system, a process that favours opportunistic phytoplankton (Tsakalakis et al., 2018). Here, we have shown that this mechanism persists in a global ocean model that resolves several realistic features of marine ecosystems, such as resource competition in the water column, multi-nutrient limitation, spatial and temporal variation of resource supply and zooplankton predation.

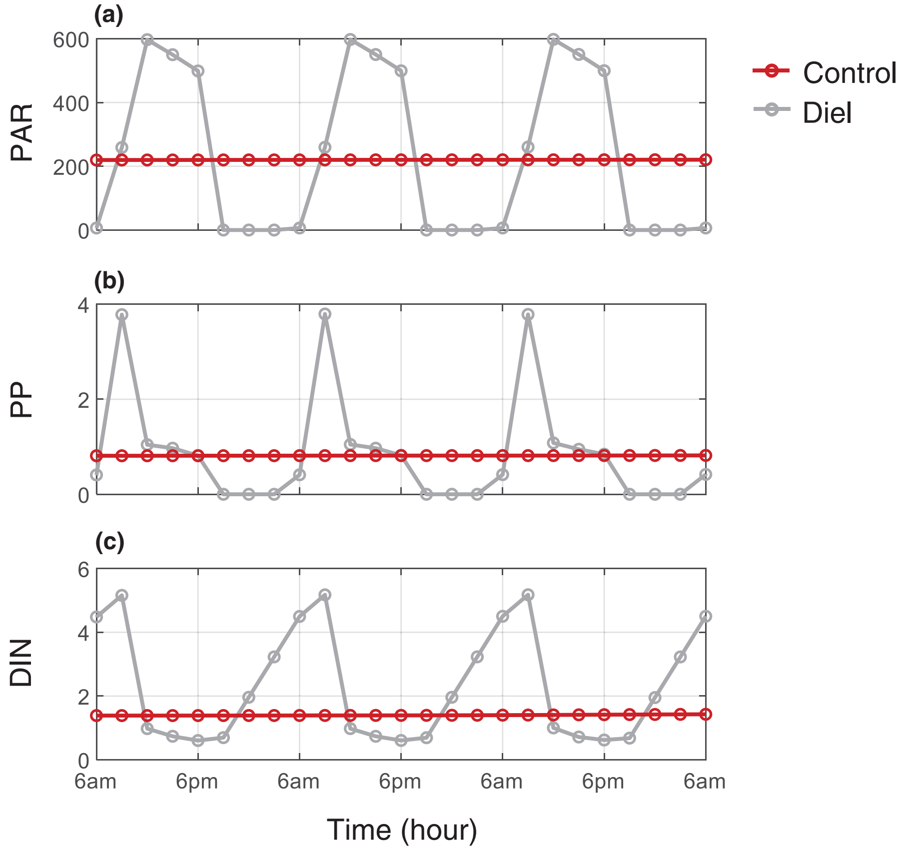

FIGURE 3 Diel dynamics in the control (red) and diel (grey) simulations of the surface ocean (0–55 m depth) for 3 days, 1–3 April, at the tropical location L2. (a) Photosynthetically active radiation (PAR; in microensteins per metre squared per second). (b) Primary production (PP; in nanomoles of carbon per metre cubed per second). (c) Dissolved inorganic nitrogen (DIN) = $NO_3^- + NO_2^- + NH_4^+$ (in micromoles of nitrogen per metre cubed). Circles indicate the model time step of three hours.

Diel nutrient cycles in our model are caused by increases during the night owing to remineralization and decreases in the day owing to uptake. In the control simulation, limiting nutrients are maintained at low concentrations in tropics because the weak seasonality allows phytoplankton to deplete limiting nutrients throughout the year. In such conditions, gleaner types dominate owing to their high nutrient affinity compared with other strategies (lowest R*, following terminology of Tilman, 1982). Addition of diel light cycles induces diel nutrient cycles that increase the relative abundance of fast-growing phytoplankton, especially at low latitudes of weak seasonality. However, there might be other processes that can potentially affect the amplitude of diel nutrient cycles. These might include diel patterns in nutrient competition between phytoplankton and bacteria (Follett et al., 2022; Kirchman et al., 1994) or diel variations in remineralization rates (Graham et al., 2000) that are not included in the present model.

The amplitude of diel nutrient oscillations in our model is ≤0.1 mmol N/m^3 for DIN, 8×10^{-3} mmol P/m^3 for phosphate and 5×10^{-6} mmol Fe/m^3 for iron. Those oscillations seem small in comparison to seasonal nutrient variations; however, our model analysis shows that they affect phytoplankton competition significantly at low latitudes, where limiting nutrients are at low concentrations throughout the year.

It is important to validate modelled diel nutrient cycles against ocean observations, but such high-frequency data are very sparse. The lack of data is because concentrations of limiting nutrients are often at undetectable levels, especially in low-latitude regions, where the diel effect is more important. However, diel cycles in nitrate concentrations have been captured using automated measuring methods in coastal ecosystems (Johnson et al., 2006; Sakamoto et al., 2017) and the open ocean (Johnson et al., 2013; Zhang et al., 2001). The study by Zhang et al. (2001) in a marine anticyclonic eddy in the North Atlantic shows that surface nitrate concentration oscillates with an amplitude of 0.045 mmol N/m^3, peaking at night and declining during the day, supporting the mechanism proposed in our study (Figure 3). The area studied by Zhang et al. (2001) is in the same region as location L4 of our analysis, where our model presents nitrate oscillations with an amplitude of 0.025 mmol N/m^3 during the same time period (Figure 2e4), showing that our model underestimates the amplitude in that case. This indicates that the effect of diel cycles on phytoplankton competition might be even stronger than our current model predictions, but more observations at several ocean locations are needed for model validation.

Our model also predicts diel cycles in phytoplankton populations, especially at low latitudes, where seasonal dynamics are weak. Observations confirm that the biomass of marine

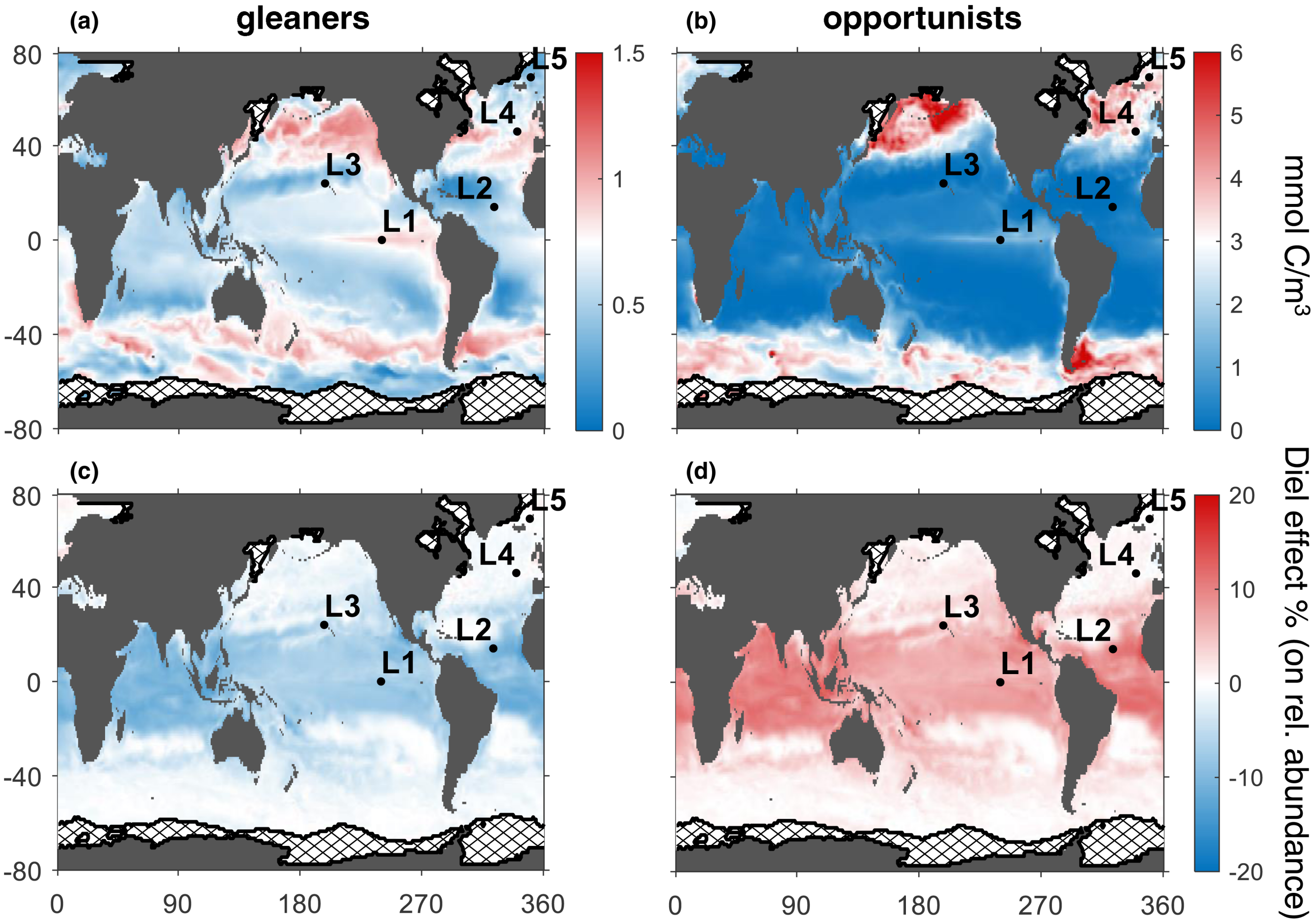

FIGURE 4 Effect of diel light cycles on phytoplankton biogeography. (a,b) Annually averaged surface concentrations (0–55 m depth) of (a) gleaners and (b) opportunists in the control simulation. (c,d) Effect of diel light cycles on the relative abundances (Equation 2; difference in relative concentrations between diel and control simulations, expressed as a percentage) of (c) gleaners and (d) opportunists. Labelled black dots indicate locations (L1–L5) for which dynamics are presented in Figure 2. White with cross-hatching indicates areas with the presence of ice.

phytoplankton oscillates with a diel pattern (Boysen et al., 2020; Fuhrman et al., 1985; Ribalet et al., 2015; Stramska & Dickey, 1992). The study by Boysen et al. (2020) captures diel cycles in pico-phytoplankton populations (*Prochlorococcus* sp., *Synechococcus* sp. and pico-eukaryotes) near Hawaii, which is close to our location L1 (Figure 3), and the four smallest phytoplankton types in our model (gleaners) correspond to a *Prochlorococcus* type, a *Synechococcus* type and two types representing pico-eukaryotes. Boysen et al. (2020) report diel population cycles with an amplitude up to *c.* 0.125 mmol C/m^3 for *Prochlorococcus* sp., *c.* 0.008 mmol C/m^3 for *Synechococcus* sp. and *c.* 0.08 mmol C/m^3 for pico-eukaryotes, and for the same functional groups our model predicts amplitudes of 0.13, 0.1 and 0.1 mmol C/m^3, respectively. Although our model overestimates the amplitude of diel cycles in *Synechococcus* sp., it does capture the amplitude of the diel population cycles for *Prochlorococcus* sp. and pico-eukaryotes.

The model suggests that diel light cycles significantly affect phytoplankton biogeography by increasing the biomass of opportunistic phytoplankton at low latitudes; the smallest size classes of opportunists (range of nano-phytoplankton) are favoured the most, because they have the highest maximal specific growth rates among those size classes. Phytoplankton competition in low-latitude oceans inferred by remote-sensing observations indicates that pico-phytoplankton (such as *Prochlorococcus* sp.) dominate at subtropical oligotrophic gyres, whereas nano-phytoplankton (such as diatoms) dominate in more productive tropical waters (Bracher et al., 2009; Brewin et al., 2010; Hirata et al., 2011). Previous modelling studies have shown that resistance to predation might be a trait explaining the presence, but not dominance, of nano-phytoplankton at low latitudes (Prowe et al., 2012; Ward et al., 2012). Our study highlights an additional and potential bottom-up mechanism at low latitudes that increases the competitive ability of opportunistic phytoplankton.

Furthermore, the model shows that diel light cycles might affect the differences in biogeography among pico-phytoplankton populations. The largest gleaners, which have the highest maximal specific growth rate among members of the gleaner group in our model, increase their abundance at low latitudes when diel light cycles are added to the model (Figure 5a,b). This information is relevant for biogeography studies of keystone pico-phytoplankton populations,

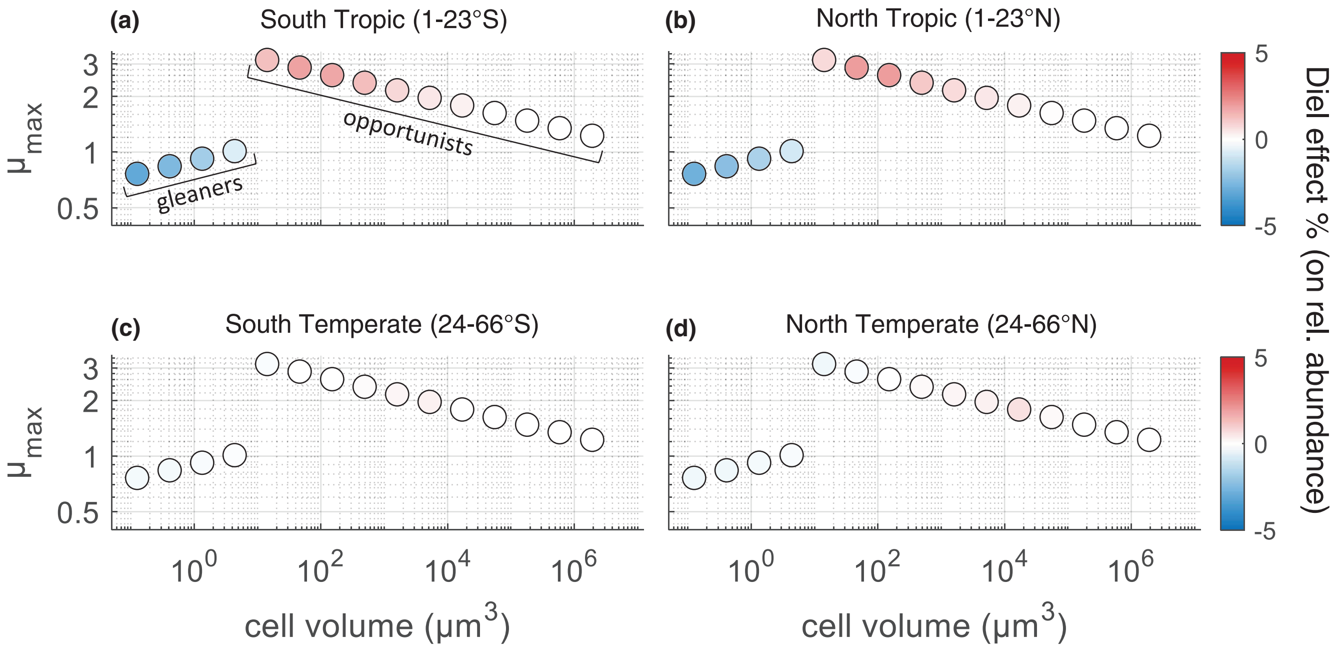

FIGURE 5 Effect of diel light cycles on phytoplankton cell size in: (a,b) tropical and (c,d) temperate oceans. The 15 modelled phytoplankton types are shown (circles) as a function of their maximal growth rate (μ_{max}, per day) of the control simulation versus cell volume. Colouring refers to the effect of diel light cycles on relative abundance (Equation 2; difference in relative concentrations between diel and control simulations, expressed as a percentage) of each phytoplankton type in the surface (0–55 m depth) of the respective latitudinal region. Phytoplankton groups of gleaners and opportunists are annotated in (a).

such as *Prochlorococcus* sp. versus *Synechococcus* sp. (Flombaum et al., 2013), or ecotypes of *Prochlorococcus* sp. (Martiny et al., 2009). Our work indicates that phytoplankton gleaners with higher maximal specific growth rates might be favoured by diel nutrient cycles in low-latitude oceans.

4.1 | Future perspectives

The best approach to estimate the impact of diel light cycles in the global ocean would be to develop a model with experimentally derived growth parameters of phytoplankton in diel oscillating conditions. Although there are meta-analysis studies determining growth parameters of several phytoplankton (Edwards et al., 2012, 2015; Finkel et al., 2010), maximal growth rates are typically estimated per day, hence ignoring the impact of diel cycles. Our analysis shows that when accounting for diel light cycles, the maximal growth rate of phytoplankton should be roughly doubled to produce levels of ocean primary production found using the daily averaged growth rate (Supporting information Figure S1), a result that has been shown before (Goebel et al., 2010). This is understandable, because diel light cycles require phytoplankton to photosynthesize only during the daytime, which is roughly half of the day, compared with conditions of averaged diel light input that are used in most ocean models. Our work indicates that laboratory studies characterizing the diel cycle of growth rates, together with monitoring dynamics of light and limiting nutrients, could inform future ocean models that resolve diel processes.

A relevant extension of the proposed model is to include nutrient storage by phytoplankton with the use of a cell-quota model (e.g., Ward et al., 2012). In the Monod model used here, photosynthesis and nutrient uptake are coupled; carbon and nutrients are instantly converted into biomass when they are both taken up by phytoplankton. Therefore, in a model resolving diel light cycles, uptake of nutrients is possible only during the day. Nutrient uptake by phytoplankton is often found to be significantly higher during the day than at night (Cochlan et al., 1991; Glibert & Garside, 1992; Yingling et al., 2021), hence a Monod model seems relevant to capture the general diel dynamics. However, studies have shown that some phytoplankton continue to take up nutrients during nighttime and store them in internal nutrient pools (Follett, White, et al., 2018; Needoba & Harrison, 2004), and large phytoplankton have significantly larger internal nutrient pools than smaller cells (Marañón et al., 2013). This indicates that the diel cycle might help to explain the presence of large phytoplankton specializing in storage of nutrients during the nighttime. We could speculate that if storage is a key adaptation to the diel nutrient cycle, nutrient oscillations in the water column should be dampened and replaced by strong oscillations in the cell quota of phytoplankton.

The circadian clock is also a well-known trait improving the fitness of microbes under diel light cycles (Johnson et al., 2017; Kolody et al., 2019), which can be either strongly present in some phytoplankton species (Cohen & Golden, 2015) or absent in others (Holtzendorff et al., 2008). This suggests that some phytoplankton might depend strongly on the diel cycle for their survival or competitiveness, whereas others do not. A recent study shows that the circadian clock and nutrient storage both increase energy acquisition by phytoplankton growing in a chemostat model under diel light cycles (Vallino & Tsakalakis, 2020), supporting the potential of those traits to affect phytoplankton competition and biogeography in the global ocean.

ACKNOWLEDGMENTS

We would like to thank Oliver Jahn for his help with model simulations. Simons Collaboration on Computational Biogeochemical Modeling of Marine Ecosystems supported M.J.F. and S.D. on CBIOMES grant #549931; C.L.F. on CBIOMES grants #827829 and #553242; and J.J.V. and I.T. on CBIOMES grant #549941. The National Science Foundation supported I.T. and J.J.V. on award #1558710 and J.J.V. on awards #1637630, #1655552 and #1841599.

CONFLICT OF INTEREST

None.

DATA AVAILABILITY STATEMENT

The data that support the findings of this study are openly available in “Global ocean model results—effects of diel light cycles” at: https://doi.org/10.5281/zenodo.6426360.

ORCID

Ioannis Tsakalakis https://orcid.org/0000-0002-1693-5383

REFERENCES

Acevedo-Trejos, E., Brandt, G., Merico, A., & Smith, S. L. (2013). Biogeographical patterns of phytoplankton community size structure in the oceans. *Global Ecology and Biogeography*, *22*, 1060–1070. https://doi.org/10.1111/geb.12071

Aumont, O., Maier-Reimer, E., Blain, S., & Monfray, P. (2003). An ecosystem model of the global ocean including Fe, Si, P colimitations. *Global Biogeochemical Cycles*, *17*, 1–15. https://doi.org/10.1029/2001GB001745

Barton, A. D., Dutkiewicz, S., Flierl, G., Bragg, J., & Follows, M. J. (2010). Patterns of diversity in marine phytoplankton. *Science*, *327*, 1509–1511. https://doi.org/10.1126/science.1184961

Barton, A. D., Pershing, A. J., Litchman, E., Record, N. R., Edwards, K. F., Finkel, Z. V., Kiørboe, T., & Ward, B. A. (2013). The biogeography of marine plankton traits. *Ecology Letters*, *16*, 522–534. https://doi.org/10.1111/ele.12063

Behrenfeld, M. J., & Boss, E. S. (2014). Resurrecting the ecological underpinnings of ocean plankton blooms. *Annual Review of Marine Science*, *6*, 167–194. https://doi.org/10.1146/annurev-marine-052913-021325

Boysen, A. K., Carlson, L. T., Durham, B. P., Groussman, R. D., Aylward, F. O., Ribalet, F., Heal, K. R., DeLong, E. F., Armbrust, E. V., & Ingalls, A. E. (2020). Diel oscillations of particulate metabolites reflect synchronized microbial activity in the North Pacific Subtropical Gyre. bioRxiv 2020.05.09.086173. https://doi.org/10.1101/2020.05.09.086173

Bracher, A., Vountas, M., Dinter, T., Burrows, J. P., Röttgers, R., & Peeken, I. (2009). Quantitative observation of cyanobacteria and diatoms from space using PhytoDOAS on SCIAMACHY data. *Biogeosciences*, *6*, 751–764. https://doi.org/10.5194/bg-6-751-2009

Brewin, R. J. W., Sathyendranath, S., Hirata, T., Lavender, S. J., Barciela, R. M., & Hardman-Mountford, N. J. (2010). A three-component model of phytoplankton size class for the Atlantic Ocean. *Ecological Modelling*, *221*, 1472–1483. https://doi.org/10.1016/j.ecolmodel.2010.02.014

Brock, T. D. (1981). Calculating solar radiation for ecological studies. *Ecological Modelling*, *14*, 1–19. https://doi.org/10.1016/0304-3800(81)90011-9

Chai, F., Jiang, M.-S., Chao, Y., Dugdale, R. C., Chavez, F., & Barber, R. T. (2007). Modeling responses of diatom productivity and biogenic silica export to iron enrichment in the equatorial Pacific Ocean. *Global Biogeochemical Cycles*, *21*, 1–16. https://doi.org/10.1029/2006GB002804

Cochlan, W. P., Harrison, P. J., & Denman, K. L. (1991). Diel periodicity of nitrogen uptake by marine phytoplankton in nitrate-rich environments. *Limnology and Oceanography*, *36*, 1689–1700. https://doi.org/10.4319/lo.1991.36.8.1689

Cohen, S. E., & Golden, S. S. (2015). Circadian rhythms in cyanobacteria. *Microbiology and Molecular Biology Reviews*, *79*, 373–385. https://doi.org/10.1128/MMBR.00036-15

Denny, M. (2017). The fallacy of the average: on the ubiquity, utility and continuing novelty of Jensen's inequality. *Journal of Experimental Biology*, *220*, 139–146. https://doi.org/10.1242/jeb.140368

Dutkiewicz, S., Boyd, P. W., & Riebesell, U. (2021). Exploring biogeochemical and ecological redundancy in phytoplankton communities in the global ocean. *Global Change Biology*, *27*, 1196–1213. https://doi.org/10.1111/gcb.15493

Dutkiewicz, S., Cermeno, P., Jahn, O., Follows, M. J., Hickman, A. E., Taniguchi, D. A. A., & Ward, B. A. (2020). Dimensions of marine phytoplankton diversity. *Biogeosciences*, *17*, 609–634. https://doi.org/10.5194/bg-17-609-2020

Dutkiewicz, S., Follows, M. J., & Bragg, J. G. (2009). Modeling the coupling of ocean ecology and biogeochemistry. *Global Biogeochemical Cycles*, *23*, GB4017. https://doi.org/10.1029/2008GB003405

Dutkiewicz, S., Hickman, A. E., Jahn, O., Henson, S., Beaulieu, C., & Monier, E. (2019). Ocean colour signature of climate change. *Nature Communications*, *10*, 1–13. https://doi.org/10.1038/s41467-019-08457-x

Dutkiewicz, S., Morris, J. J., Follows, M. J., Scott, J., Levitan, O., Dyhrman, S. T., & Berman-Frank, I. (2015). Impact of ocean acidification on the structure of future phytoplankton communities. *Nature Climate Change*, *5*, 1002–1006. https://doi.org/10.1038/nclimate2722

Dutkiewicz, S., Ward, B. A., Scott, J. R., & Follows, M. J. (2014). Understanding predicted shifts in diazotroph biogeography using resource competition theory. *Biogeosciences*, *11*, 5445–5461. https://doi.org/10.5194/bg-11-5445-2014

Edwards, K. F., Thomas, M. K., Klausmeier, C. A., & Litchman, E. (2012). Allometric scaling and taxonomic variation in nutrient utilization traits and maximum growth rate of phytoplankton. *Limnology and Oceanography*, *57*, 554–566. https://doi.org/10.4319/lo.2012.57.2.0554

Edwards, K. F., Thomas, M. K., Klausmeier, C. A., & Litchman, E. (2015). Light and growth in marine phytoplankton: allometric, taxonomic, and environmental variation. *Limnology and Oceanography*, *60*, 540–552. https://doi.org/10.1002/lno.10033

Finkel, Z. V., Beardall, J., Flynn, K. J., Quigg, A., Rees, T. A. V., & Raven, J. A. (2010). Phytoplankton in a changing world: cell size and elemental stoichiometry. *Journal of Plankton Research*, *32*, 119–137. https://doi.org/10.1093/plankt/fbp098

Flombaum, P., Gallegos, J. L., Gordillo, R. A., Rincón, J., Zabala, L. L., Jiao, N., Karl, D. M., Li, W. K. W., Lomas, M. W., Veneziano, D., Vera, C. S., Vrugt, J. A., & Martiny, A. C. (2013). Present and future global distributions of the marine Cyanobacteria Prochlorococcus and Synechococcus. *Proceedings of the National Academy of Sciences*, *110*, 9824–9829. https://doi.org/10.1073/pnas.1307701110

Follett, C. L., Dutkiewicz, S., Karl, D. M., Inomura, K., & Follows, M. J. (2018). Seasonal resource conditions favor a summertime increase in North Pacific diatom–diazotroph associations. *The ISME Journal*, *12*, 1543–1557. https://doi.org/10.1038/s41396-017-0012-x

Follett, C. L., Dutkiewicz, S., Ribalet, F., Zakem, E., Caron, D., Armbrust, E. V., & Follows, M. J. (2022). Trophic interactions with heterotrophic bacteria limit the range of Prochlorococcus. *Proceedings of the National Academy of Sciences*, *119*, e2110993118. https://doi.org/10.1073/pnas.2110993118

Follett, C. L., White, A. E., Wilson, S. T., & Follows, M. J. (2018). Nitrogen fixation rates diagnosed from diurnal changes in elemental stoichiometry. *Limnology and Oceanography*, *63*, 1911–1923. https://doi.org/10.1002/lno.10815

Follows, M. J., & Dutkiewicz, S. (2011). Modeling diverse communities of marine microbes. *Annual Review of Marine Science*, *3*, 427–451. https://doi.org/10.1146/annurev-marine-120709-142848

Follows, M. J., Dutkiewicz, S., Grant, S., & Chisholm, S. W. (2007). Emergent biogeography of microbial communities in a model ocean. *Science*, *315*, 1843–1846. https://doi.org/10.1126/science.1138544

Fuhrman, J. A., Eppley, R. W., Hagström, Å., & Azam, F. (1985). Diel variations in bacterioplankton, phytoplankton, and related parameters in the Southern California Bight. *Marine Ecology Progress Series*, *27*, 9–20.

Geider, R. J., MacIntyre, H. L., & Kana, T. M. (1998). A dynamic regulatory model of phytoplanktonic acclimation to light, nutrients, and temperature. *Limnology and Oceanography*, *43*, 679–694. https://doi.org/10.4319/lo.1998.43.4.0679

Glibert, P. M., & Garside, C. (1992). Diel variability in nitrogenous nutrient uptake by phytoplankton in the Chesapeake Bay plume. *Journal of Plankton Research*, *14*, 271–288. https://doi.org/10.1093/plankt/14.2.271

Goebel, N. L., Edwards, C. A., Zehr, J. P., & Follows, M. J. (2010). An emergent community ecosystem model applied to the California Current System. *Journal of Marine Systems*, *83*, 221–241. https://doi.org/10.1016/j.jmarsys.2010.05.002

Graham, W. M., MacIntyre, S., & Alldredge, A. L. (2000). Diel variations of marine snow concentration in surface waters and implications for particle flux in the sea. *Deep Sea Research Part I: Oceanographic Research Papers*, *47*, 367–395. https://doi.org/10.1016/S0967-0637(99)00063-1

Grover, J. P. (1990). Resource competition in a variable environment: Phytoplankton growing according to Monod's model. *The American Naturalist*, *136*, 771–789.

Hansen, P. J., Bjørnsen, P. K., & Hansen, B. W. (1997). Zooplankton grazing and growth: Scaling within the 2-2,-μm body size range. *Limnology and Oceanography*, *42*, 687–704. https://doi.org/10.4319/lo.1997.42.4.0687

Hirata, T., Hardman-Mountford, N. J., Brewin, R. J. W., Aiken, J., Barlow, R., Suzuki, K., Isada, T., Howell, E., Hashioka, T., Noguchi-Aita, M., & Yamanaka, Y. (2011). Synoptic relationships between surface Chlorophyll-a and diagnostic pigments specific to phytoplankton functional types. *Biogeosciences*, *8*, 311–327. https://doi.org/10.5194/bg-8-311-2011

Holling, C. S. (1959). Some characteristics of simple types of predation and parasitism1. *The Canadian Entomologist*, *91*, 385–398. https://doi.org/10.4039/Ent91385-7

Holtzendorff, J., Partensky, F., Mella, D., Lennon, J.-F., Hess, W. R., & Garczarek, L. (2008). Genome streamlining results in loss of robustness of the circadian clock in the marine cyanobacterium Prochlorococcus marinus PCC 9511. *Journal of Biological Rhythms*, *23*, 187–199. https://doi.org/10.1177/0748730408316040

Jensen, J. L. W. V. (1906). Sur les fonctions convexes et les inégalités entre les valeurs moyennes. *Acta Mathematica*, *30*, 175–193. https://doi.org/10.1007/BF02418571

Johnson, C. H., Zhao, C., Xu, Y., & Mori, T. (2017). Timing the day: What makes bacterial clocks tick? *Nature Reviews Microbiology*, *15*, 232–242. https://doi.org/10.1038/nrmicro.2016.196

Johnson, K. S., Coletti, L. J., & Chavez, F. P. (2006). Diel nitrate cycles observed with in situ sensors predict monthly and annual new production. *Deep Sea Research Part I: Oceanographic Research Papers*, *53*, 561–573. https://doi.org/10.1016/j.dsr.2005.12.004

Johnson, K. S., Coletti, L. J., Jannasch, H. W., Sakamoto, C. M., Swift, D. D., & Riser, S. C. (2013). Long-term nitrate measurements in the ocean using the in situ ultraviolet spectrophotometer: Sensor integration into the APEX profiling float. *Journal of Atmospheric and Oceanic Technology*, *30*, 1854–1866. https://doi.org/10.1175/JTECH-D-12-00221.1

Kiørboe, T. (1993). Turbulence, phytoplankton cell size, and the structure of pelagic food webs. In J. H. S. Blaxter & A. J. Southward (Eds.), *Advances in marine biology* (pp. 1–72). Academic Press. https://doi.org/10.1016/S0065-2881(08)60129-7

Kirchman, D. L., Ducklow, H. W., McCarthy, J. J., & Garside, C. (1994). Biomass and nitrogen uptake by heterotrophic bacteria during the spring phytoplankton bloom in the North Atlantic Ocean. *Deep Sea Research Part I: Oceanographic Research Papers*, *41*, 879–895. https://doi.org/10.1016/0967-0637(94)90081-7

Kolody, B. C., McCrow, J. P., Allen, L. Z., Aylward, F. O., Fontanez, K. M., Moustafa, A., Moniruzzaman, M., Chavez, F. P., Scholin, C. A., Allen, E. E., Worden, A. Z., Delong, E. F., & Allen, A. E. (2019). Diel transcriptional response of a California Current plankton microbiome to light, low iron, and enduring viral infection. *The ISME Journal*, *13*, 2817–2833. https://doi.org/10.1038/s41396-019-0472-2

Landolfi, A., Koeve, W., Dietze, H., Kähler, P., & Oschlies, A. (2015). A new perspective on environmental controls of marine nitrogen fixation. *Geophysical Research Letters*, *42*, 4482–4489. https://doi.org/10.1002/2015GL063756

Litchman, E. (1998). Population and community responses of phytoplankton to fluctuating light. *Oecologia*, *117*, 247–257. https://doi.org/10.1007/s004420050655

Litchman, E. (2003). Competition and coexistence of phytoplankton under fluctuating light: Experiments with two cyanobacteria. *Aquatic Microbial Ecology*, *31*, 241–248. https://doi.org/10.3354/ame031241

Litchman, E., & Klausmeier, C. A. (2001). Competition of phytoplankton under fluctuating light. *The American Naturalist*, *157*, 170–187.

Litchman, E., & Klausmeier, C. A. (2008). Trait-based community ecology of phytoplankton. *Annual Review of Ecology, Evolution, and Systematics*, *39*, 615–639.

Litchman, E., Klausmeier, C. A., & Bossard, P. (2004). Phytoplankton nutrient competition under dynamic light regimes. *Limnology and Oceanography*, *49*, 1457–1462. https://doi.org/10.4319/lo.2004.49.4_part_2.1457

Marañón, E., Cermeño, P., López-Sandoval, D. C., Rodríguez-Ramos, T., Sobrino, C., Huete-Ortega, M., Blanco, J. M., & Rodríguez, J. (2013). Unimodal size scaling of phytoplankton growth and the size dependence of nutrient uptake and use. *Ecology Letters*, *16*, 371–379. https://doi.org/10.1111/ele.12052

Marshall, J., Adcroft, A., Hill, C., Perelman, L., & Heisey, C. (1997). A finite-volume, incompressible Navier Stokes model for studies of the ocean on parallel computers. *Journal of Geophysical Research: Oceans*, *102*, 5753–5766. https://doi.org/10.1029/96JC02775

Martiny, A. C., Tai, A. P. K., Veneziano, D., Primeau, F., & Chisholm, S. W. (2009). Taxonomic resolution, ecotypes and the biogeography of Prochlorococcus. *Environmental Microbiology*, *11*, 823–832. https://doi.org/10.1111/j.1462-2920.2008.01803.x

Monod, J. (1949). The growth of bacterial cultures. *Annual Review of Microbiology*, *3*, 371–394. https://doi.org/10.1146/annurev.mi.03.100149.002103

Monteiro, F. M., Follows, M. J., & Dutkiewicz, S. (2010). Distribution of diverse nitrogen fixers in the global ocean. *Global Biogeochemical Cycles*, *24*, 1–16. https://doi.org/10.1029/2009GB003731

Needoba, J. A., & Harrison, P. J. (2004). Influence of low light and a light: Dark cycle on no3– uptake, intracellular no3–, and nitrogen isotope fractionation by marine phytoplankton1. *Journal of Phycology*, *40*, 505–516. https://doi.org/10.1111/j.1529-8817.2004.03171.x

Prowe, A. E. F., Pahlow, M., Dutkiewicz, S., Follows, M., & Oschlies, A. (2012). Top-down control of marine phytoplankton diversity in a global ecosystem model. *Progress in Oceanography*, *101*, 1–13. https://doi.org/10.1016/j.pocean.2011.11.016

Ptacnik, R., Solimini, A. G., Andersen, T., Tamminen, T., Brettum, P., Lepistö, L., Willén, E., & Rekolainen, S. (2008). Diversity predicts stability and resource use efficiency in natural phytoplankton communities. *Proceedings of the National Academy of Sciences*, *105*, 5134–5138. https://doi.org/10.1073/pnas.0708328105

Raven, J. A. (1994). Why are there no picoplanktonic O2 evolvers with volumes less than 10–19 m3? *Journal of Plankton Research*, *16*, 565–580. https://doi.org/10.1093/plankt/16.5.565

Ribalet, F., Swalwell, J., Clayton, S., Jiménez, V., Sudek, S., Lin, Y., Johnson, Z. I., Worden, A. Z., & Armbrust, E. V. (2015). Light-driven synchrony of Prochlorococcus growth and mortality in the subtropical Pacific gyre. *Proceedings of the National Academy of Sciences*, *112*, 8008–8012. https://doi.org/10.1073/pnas.1424279112

Sakamoto, C. M., Johnson, K. S., Coletti, L. J., Maurer, T. L., Massion, G., Pennington, J. T., Plant, J. N., Jannasch, H. W., & Chavez, F. P. (2017). Hourly in situ nitrate on a coastal mooring: A 15-year record and insights into new production. *Oceanography*, *30*, 114–127.

Sommer, U., Adrian, R., Domis, L. D. S., Elser, J. J., Gaedke, U., Ibelings, B., Jeppesen, E., Lürling, M., Molinero, J. C., Mooij, W. M., van Donk, E., & Winder, M. (2012). Beyond the Plankton Ecology Group (PEG) model: Mechanisms driving plankton succession. *Annual Review of Ecology, Evolution, and Systematics*, *43*, 429–448. https://doi.org/10.1146/annurev-ecolsys-110411-160251

Sommer, U., Charalampous, E., Genitsaris, S., & Moustaka-Gouni, M. (2017). Benefits, costs and taxonomic distribution of marine phytoplankton body size. *Journal of Plankton Research*, *39*, 494–508. https://doi.org/10.1093/plankt/fbw071

Stramska, M., & Dickey, T. D. (1992). Variability of bio-optical properties of the upper ocean associated with diel cycles in phytoplankton population. *Journal of Geophysical Research: Oceans*, *97*, 17873–17887. https://doi.org/10.1029/92JC01570

Thomas, D. N. (2003). Iron limitation in the Southern Ocean. *Science*, *302*, 565–566. https://doi.org/10.1126/science.302.5645.565c

Tilman, D. (1982). *Resource competition and community structure*. Princeton University Press.

Tréguer, P., Bowler, C., Moriceau, B., Dutkiewicz, S., Gehlen, M., Aumont, O., Bittner, L., Dugdale, R., Finkel, Z., Iudicone, D., Jahn, O., Guidi, L., Lasbleiz, M., Leblanc, K., Levy, M., & Pondaven, P. (2018). Influence of diatom diversity on the ocean biological carbon pump. *Nature Geoscience*, *11*, 27–37. https://doi.org/10.1038/s41561-017-0028-x

Tsakalakis, I., Follows, M. J., Dutkiewicz, S., Follett, C. L., & Vallino, J. J. (2021). *Global ocean model results—Effects of diel light cycles*. Zenodo. https://doi.org/10.5281/zenodo.6426360

Tsakalakis, I., Pahlow, M., Oschlies, A., Blasius, B., & Ryabov, A. B. (2018). Diel light cycle as a key factor for modelling phytoplankton biogeography and diversity. *Ecological Modelling*, *384*, 241–248. https://doi.org/10.1016/j.ecolmodel.2018.06.022

Vallina, S. M., Follows, M. J., Dutkiewicz, S., Montoya, J. M., Cermeno, P., & Loreau, M. (2014). Global relationship between phytoplankton diversity and productivity in the ocean. *Nature Communications*, *5*, 1–10. https://doi.org/10.1038/ncomms5299

Vallino, J. J., & Tsakalakis, I. (2020). Phytoplankton temporal strategies increase entropy production in a marine food web model. *Entropy*, *22*, 1249. https://doi.org/10.3390/e22111249

Ward, B. A., Dutkiewicz, S., Jahn, O., & Follows, M. J. (2012). A size-structured food-web model for the global ocean. *Limnology and Oceanography*, *57*, 1877–1891. https://doi.org/10.4319/lo.2012.57.6.1877

Ward, B. A., & Follows, M. J. (2016). Marine mixotrophy increases trophic transfer efficiency, mean organism size, and vertical carbon flux. *Proceedings of the National Academy of Sciences*, *113*, 2958–2963. https://doi.org/10.1073/pnas.1517118113

Winder, M., & Sommer, U. (2012). Phytoplankton response to a changing climate. *Hydrobiologia*, *698*, 5–16. https://doi.org/10.1007/s10750-012-1149-2

Wunsch, C., & Heimbach, P. (2007). Practical global oceanic state estimation. *Physica D: Nonlinear Phenomena, Data Assimilation*, *230*, 197–208. https://doi.org/10.1016/j.physd.2006.09.040

Yingling, N., Kelly, T. B., Shropshire, T. A., Landry, M. R., Selph, K. E., Knapp, A. N., Kranz, S. A., & Stukel, M. R. (2021). Taxon-specific phytoplankton growth, nutrient utilization, and light limitation in the oligotrophic Gulf of Mexico. bioRxiv 2021.03.01.433426. https://doi.org/10.1101/2021.03.01.433426

Zhang, J.-Z., Wanninkhof, R., & Lee, K. (2001). Enhanced new production observed from the diurnal cycle of nitrate in an oligotrophic anticyclonic eddy. *Geophysical Research Letters*, *28*, 1579–1582. https://doi.org/10.1029/2000GL012065

BIOSKETCH

Ioannis Tsakalakis is an ocean modeller using simple conceptual models and global ocean simulations to understand the underlying mechanisms that govern macroecological patterns in the global ocean. His research is focused on phytoplankton, because their role is crucial for predicting ocean productivity, biogeochemical cycles and the climate of the Earth. He parameterizes models with experimentally derived growth parameters of phytoplankton and interprets model results against experimental data and in situ and remote-sensing observations. He seeks to determine the key environmental factors that explain the realized niche and biogeography of keystone phytoplankton functional groups, such as small cyanobacteria, diatoms and dinoflagellates, and biodiversity patterns in the global ocean.

SUPPORTING INFORMATION

Additional supporting information can be found online in the Supporting Information section at the end of this article.

How to cite this article: Tsakalakis, I., Follows, M. J., Dutkiewicz, S., Follett, C. L., & Vallino, J. J. (2022). Diel light cycles affect phytoplankton competition in the global ocean. *Global Ecology and Biogeography*, *31*, 1838–1849. https://doi.org/10.1111/geb.13562